

Numerical analysis of tissue heating using the bioheat transfer porous model

Ewa Majchrzak, Łukasz Turchan

Institute of Computational Mechanics and Engineering

Silesian University of Technology, Konarskiego 18a, 44-100 Gliwice, Poland

e-mail: ewa.majchrzak@polsl.pl, lukasz.turchan@polsl.pl

The paper concerns the modelling of artificial hyperthermia. The 3D domain including healthy tissue and tumor region is considered. Heat transfer processes proceeding in this domain are described by the Pennes model and next by the porous one. The external heating of tissue is taken into account by the introduction of internal source function to the equation considered. Both models are supplemented by the same geometrical, physical, boundary and initial conditions. At the stage of numerical simulation the explicit scheme of finite difference method is used. The examples of computations show the similarities and differences of solutions and allow to formulate the conclusions connected with the applications of the results obtained in the hyperthermia therapy.

Keywords: bioheat transfer, heating of tissue, hyperthermia therapy, porous model, Pennes' equation.

1. INTRODUCTION

Artificial hyperthermia is the procedure of raising tissue temperature of the part or the whole body. The procedure is applied alone or as the supplementary one with various cancer treatment modalities such as radiotherapy and chemotherapy. The effectiveness of hyperthermia depends on the value of elevated temperature and the exposure time. The problem of applying the heat directly to the tumor and the ability to predict the temperature distribution are critical. Up to the present time, many different bioheat transfer models have been proposed for determining the temperature distribution in the living tissues. The most commonly used was the Pennes equation [3–5, 8, 9, 11, 15, 16, 19], although in recent years the Cattaneo-Vernotte equation [2, 6, 13, 21] or the dual-phase-lag equation [1, 10, 14, 20, 22, 24, 25] were also suggested.

The biological tissue is the material with particular nonhomogeneous inner structure and interwoven blood vessels (Fig. 1). One of the biggest problems in modeling of bioheat transfer is blood

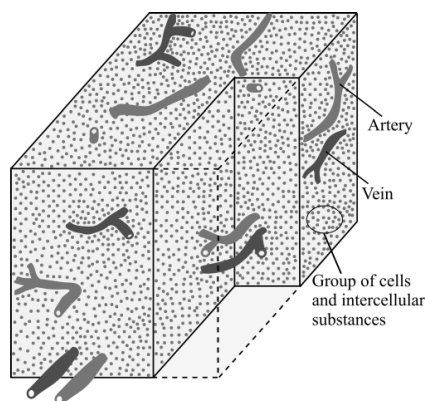


Fig. 1. Tissue model.

perfusion. The volume fraction of blood vessels in tissue and the blood velocity are very important. Thus, a natural approach seems to use the theory of porous media [7, 17] to model the temperature distribution within the tissue. Here, the model based on the theory of porous medium is considered and the results are compared with calculations obtained using the Pennes model.

2. FORMULATION OF THE PROBLEM

The domain including healthy tissue Ω_1 and the tumor region Ω_2 is a cube with the edge length of 0.05 m and the heating zone within the tumor is a centrally located cube with the edge length of 0.01 m, as shown in Fig. 2. The considered domain includes the blood vessels arranged in the direction of the x axis.

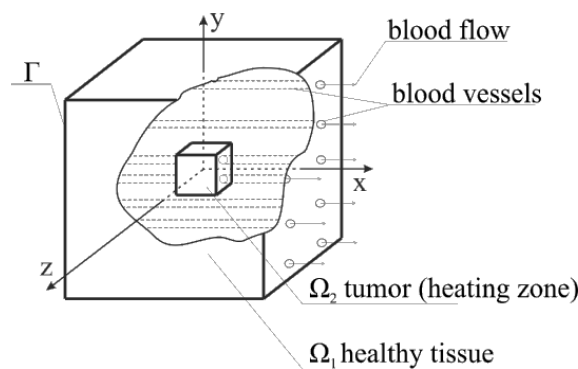


Fig. 2. Domain considered.

The Pennes equation is one of the earliest bioheat equations that describe the temperature distribution in the living tissues [8]. If the thermophysical parameters of tumor and healthy tissue are assumed to be the same, then the Pennes equation describing the temperature field in the domain considered $\Omega = \Omega_1 \cup \Omega_2$ is of the form

$$c_t \rho_t \frac{\partial T(x, y, z, t)}{\partial t} = \lambda_t \nabla^2 T(x, y, z, t) + G_b c_b \rho_b [T_B - T(x, y, z, t)] + Q_{met} + Q_{ex}(x, y, z, t), \quad (1)$$

where c_t is the specific heat of tissue, ρ_t is the density of tissue, λ_t is the thermal conductivity of tissue, T denotes tissue temperature, t is the time, G_b is the blood perfusion coefficient, c_b is the specific heat of blood, ρ_b is the density of blood, T_B is the artery temperature, Q_{met} is the metabolic heat source and $Q_{ex}(x, y, z, t)$ is the capacity of internal heat sources associated with the external heating of tissue [23]. It should be pointed out that the artery blood temperature T_B in Eq. (1) is assumed to be uniform throughout the tissue and the vein blood temperature is equal to the tissue temperature.

As previously mentioned, the tissue can be treated as a porous medium and can be divided into two regions: vascular region (blood vessel) and extravascular region (tissue) [7, 17]. To describe temperature field in the heating tissue the two-equation porous model [18] can be applied. This model consists of equation for tissue sub-domain

$$(1 - \varepsilon) c_t \rho_t \frac{\partial T_t(x, y, z, t)}{\partial t} = (1 - \varepsilon) \lambda_t \nabla^2 T_t(x, y, z, t) + \alpha A [T_b(x, y, z, t) - T_t(x, y, z, t)] + (1 - \varepsilon) Q_{met} + (1 - \varepsilon) Q_{ex}(x, y, z, t) \quad (2)$$

and equation for blood vessels sub-domain

$$\begin{aligned} \varepsilon c_b \rho_b \frac{\partial T_b(x, y, z, t)}{\partial t} + \varepsilon c_b \rho_b \mathbf{v} \cdot \nabla T_b(x, y, z, t) = \varepsilon \lambda_b \nabla^2 T_b(x, y, z, t) \\ + \alpha A [T_t(x, y, z, t) - T_b(x, y, z, t)] + \varepsilon Q_{metb} + \varepsilon Q_{ex}(x, y, z, t), \end{aligned} \quad (3)$$

where ε denotes the porosity (the ratio of blood volume to the total volume), α is the heat transfer coefficient, \mathbf{v} is the blood velocity, A is the volumetric transfer area between tissue and blood, while subscripts t and b represent tissue and blood, respectively.

When the thermal equilibrium is maintained, the temperature of tissue is equal to the temperature of blood ($T = T_t = T_b$) and then a single equation is obtained

$$\begin{aligned} [(1 - \varepsilon)c_t \rho_t + \varepsilon c_b \rho_b] \frac{\partial T(x, y, z, t)}{\partial t} + \varepsilon c_b \rho_b u \frac{\partial T(x, y, z, t)}{\partial x} \\ = [(1 - \varepsilon)\lambda_t + \varepsilon \lambda_b] \nabla^2 T(x, y, z, t) + (1 - \varepsilon)Q_{mett} + \varepsilon Q_{metb} + Q_{ex}(x, y, z, t). \end{aligned} \quad (4)$$

In Eq. (4) the directional blood flow is taken into account, this means $\mathbf{v} = [u, 0, 0]$.

It is assumed that the source function $Q_{ex}(x, y, z, t)$ has the following form [23]:

$$(x, y, z) \in \Omega_1 : Q_{ex}(x, y, z, t) = 0, \quad (5)$$

while

$$(x, y, z) \in \Omega_2 : Q_{ex}(x, y, z, t) = \begin{cases} Q_0, & t \leq t_{ex} \\ 0, & t > t_{ex} \end{cases}, \quad (6)$$

where Q_0 is the constant source function associated with external heating and t_{ex} is exposure time. Equations (1) and (4) are supplemented by boundary condition in the form of adiabatic one, this means

$$(x, y, z) \in \Gamma : -\lambda \mathbf{n} \cdot \nabla T(x, y, z, t) = 0, \quad (7)$$

where \mathbf{n} is normal outward vector. The initial condition is the following:

$$t = 0 : T(x, y, z, t) = T_p, \quad (8)$$

where T_p is the initial temperature of tissue.

3. METHOD OF SOLUTION

Equation (4) supplemented by boundary condition (7) and initial one (8) has been solved using the explicit scheme of finite difference method [12]. Taking into account the form of source function Q_{ex} , Eq. (4) can be written as follows:

$$C_e \frac{\partial T}{\partial t} + \varepsilon c_b \rho_b u \frac{\partial T}{\partial x} = \lambda_e \nabla^2 T + (1 - \varepsilon) Q_{mett} + \varepsilon Q_{metb} + Q_e, \quad (9)$$

where $T = T(x, y, z, t)$ and Q_e is the constant non-zero component only for $(x, y, z) \in \Omega_2$ and $t \leq t_{ex}$, while

$$C_e = (1 - \varepsilon)c_t \rho_t + \varepsilon c_b \rho_b \quad (10)$$

and

$$\lambda_e = (1 - \varepsilon)\lambda_t + \varepsilon \lambda_b. \quad (11)$$

Let $T^f = T(x, y, z, f\Delta t)$, where Δt is the time step. Then, for time $t^f = f\Delta t$ the following approximate form of Eq. (9) can be proposed:

$$C_e \frac{T^f - T^{f-1}}{\Delta t} = \lambda_e \nabla^2 T^{f-1} - \varepsilon c_b \rho_b u \frac{\partial T^{f-1}}{\partial x} + (1 - \varepsilon) Q_{mett} + \varepsilon Q_{metb} + Q_e^{f-1}. \quad (12)$$

The uniform grid of dimensions $n \times n \times n$ is introduced and then the difference equations for internal node (x_i, y_j, z_k) have the following form:

$$C_e \frac{T_{i,j,k}^f - T_{i,j,k}^{f-1}}{\Delta t} = \lambda_e \nabla^2 T_{i,j,k}^{f-1} - \varepsilon c_b \rho_b u \frac{T_{i+1,j,k}^{f-1} - T_{i-1,j,k}^{f-1}}{2h} + (1 - \varepsilon) Q_{mett} + \varepsilon Q_{metb} + Q_{ei,j,k}^{f-1}, \quad (13)$$

where h is the grid step, and

$$\nabla^2 T_{i,j,k}^{f-1} = \frac{T_{i-1,j,k}^{f-1} - 2T_{i,j,k}^{f-1} + T_{i+1,j,k}^{f-1}}{h^2} + \frac{T_{i,j-1,k}^{f-1} - 2T_{i,j,k}^{f-1} + T_{i,j+1,k}^{f-1}}{h^2} + \frac{T_{i,j,k-1}^{f-1} - 2T_{i,j,k}^{f-1} + T_{i,j,k+1}^{f-1}}{h^2}. \quad (14)$$

From Eq. (13) one obtains

$$T_{i,j,k}^f = \frac{C_e h^2 - 6\lambda_e \Delta t}{C_e h^2} T_{i,j,k}^{f-1} + \frac{2\lambda_e \Delta t + \varepsilon c_b \rho_b u h \Delta t}{2C_e h^2} T_{i-1,j,k}^{f-1} + \frac{2\lambda_e \Delta t - \varepsilon c_b \rho_b u h \Delta t}{2C_e h^2} T_{i+1,j,k}^{f-1} + \frac{\lambda_e \Delta t}{C_e h^2} \left(T_{i,j-1,k}^{f-1} + T_{i,j+1,k}^{f-1} + T_{i,j,k-1}^{f-1} + T_{i,j,k+1}^{f-1} \right) + \frac{\Delta t}{C_e} \left[(1 - \varepsilon) Q_{mett} + \varepsilon Q_{metb} + Q_{ei,j,k}^{f-1} \right]. \quad (15)$$

The stability criteria are as follows

$$\frac{C_e h^2 - 6\lambda_e \Delta t}{C_e h^2} \geq 0, \quad (16)$$

$$\frac{2\lambda_e \Delta t - \varepsilon c_b \rho_b u h \Delta t}{2C_e h^2} \geq 0. \quad (17)$$

In similar way one obtains the difference equations for the Pennes equation (1) and internal node (x_i, y_j, z_k)

$$T_{i,j,k}^f = \frac{c_t \rho_t h^2 - 6\lambda \Delta t - G_b c_b \rho_b \Delta t h^2}{c_t \rho_t h^2} T_{i,j,k}^{f-1} + \frac{\lambda \Delta t}{c_t \rho_t h^2} \left(T_{i-1,j,k}^{f-1} + T_{i+1,j,k}^{f-1} + T_{i,j-1,k}^{f-1} + T_{i,j+1,k}^{f-1} + T_{i,j,k-1}^{f-1} + T_{i,j,k+1}^{f-1} \right) + \frac{\Delta t}{c_t \rho_t} \left(G_b c_b \rho_b T_B + Q_{ei,j,k}^{f-1} \right). \quad (18)$$

In this case the stability criterion is in the form

$$\frac{h^2 c_t \rho_t - 6\lambda \Delta t - G_b c_b \rho_b \Delta t h^2}{h^2 c_t \rho_t} \geq 0. \quad (19)$$

4. RESULTS OF COMPUTATIONS

In numerical computations for both models the following values of parameters have been assumed: thermal conductivity of tissue and blood $\lambda_t = \lambda_b = 0.5 \text{ W/(m K)}$, specific heat of tissue $c_t = 4000 \text{ J/(kg K)}$, specific heat of blood $c_b = 3770 \text{ J/(kg K)}$, tissue density $\rho_t = 1000 \text{ kg/m}^3$, blood density $\rho_b = 1060 \text{ kg/m}^3$, perfusion coefficient $G_B = 0.0005 \text{ 1/s}$, metabolic heat source $Q_{met} = Q_{mett} = Q_{metb} = 250 \text{ W/m}^3$, blood temperature (see for example Eq. (1)) $T_B = 37^\circ\text{C}$. The initial temperature is equal to $T_p = 37^\circ\text{C}$. The number of nodes is equal to $50 \times 50 \times 50$ and time step $\Delta t = 0.05 \text{ s}$.

Three heating conditions described in Table 1 have been considered. All of these variants have the same input energy equal to 35 MJ/m^3 . In the case of the porous media model, for each variant of heating, three sets of porosity and velocity of blood have been taken into account, as shown in Table 2 [23].

Table 1. Variants of heating.

| Variant no. | Power density Q_{ex} [MW/m^3] | Heating duration t_{ex} [s] |
|-------------|--|-------------------------------|
| 1 | 7 | 5 |
| 2 | 3.5 | 10 |
| 3 | 1 | 35 |

Table 2. Sets of porosity and blood velocity [23].

| | Porosity ε | Blood velocity u [m/s] |
|-------------|------------------------|--------------------------|
| Venules | 0.1209 | 0.00066 |
| Capillaries | 0.0659 | 0.000922 |
| Arterioles | 0.0275 | 0.0037 |

In Figs. 3, 4, and 5 the temperature distributions in the central part of the cross section (plane $\{x, y\}$) for all variants of heating are shown. Differences between isotherms obtained from the Pennes

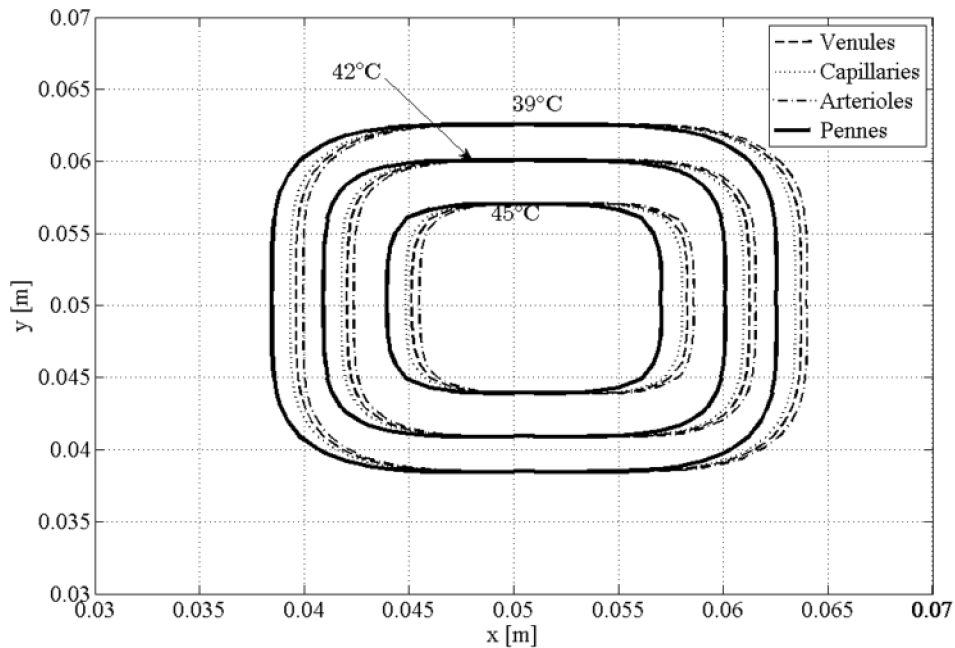


Fig. 3. Temperature distribution at the central part of cross section after 10 s – 1st variant of heating.

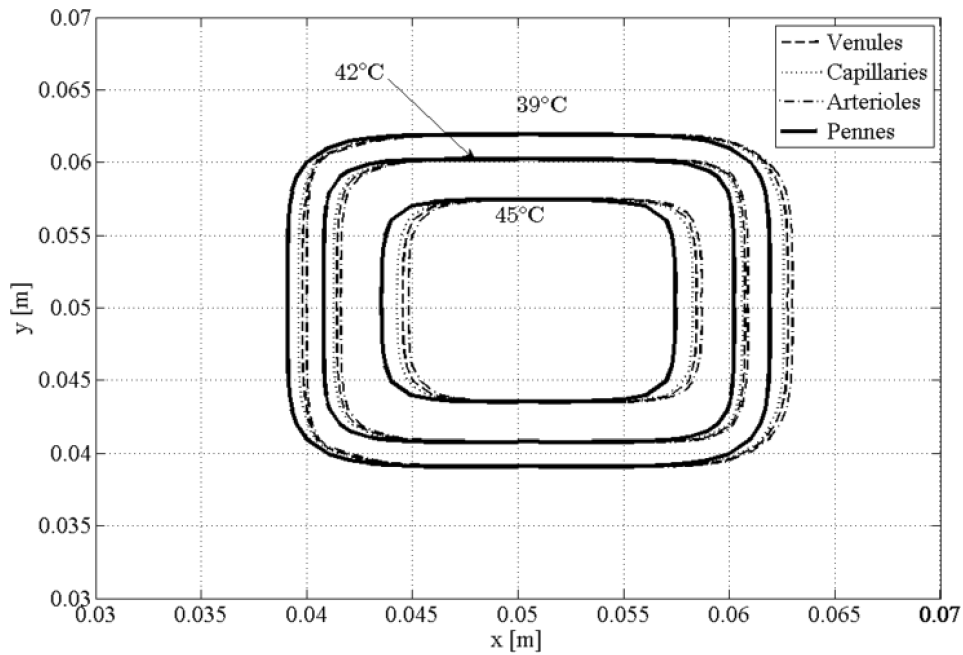


Fig. 4. Temperature distribution at the central part of cross section after 10 s – 2nd variant of heating.

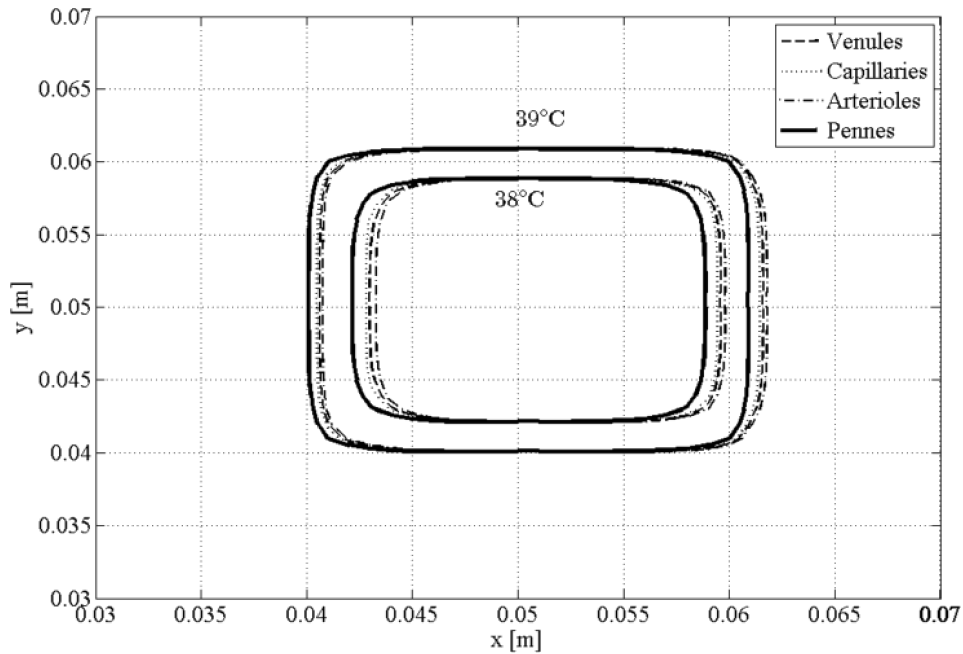


Fig. 5. Temperature distribution at the central part of cross section after 10 s – 3rd variant of heating.

equation and porous model are visible, but not too big. As can be seen, one-equation porous model brings shift of elevated temperature in direction of blood flow. This shift depends on porosity and velocity. The shift is the largest for the case with arterioles (the highest value of the product of the porosity and blood flow velocity), while the smallest shift occurs for capillaries (the smallest product of velocity and porosity). In addition, for more power and a shorter heating duration, a larger area is covered with high temperature.

Figures 6, 7 and 8 show the temperature history at the central point of the domain considered for both models. It should be noted that in the case of the porous model different types of blood vessels were taken into account. As can be seen, during heating of tissue all curves are very similar, but during cooling there are important differences. After 100 seconds the biggest differences (> 2 K) are observed between the Pennes model and porous model in which arterioles were considered. Additionally, in the case of a long heating (variant 3), the maximum tissue temperatures also differ – the highest temperature occurs with the use of Pennes model and the smallest for the porous model which takes into account arterioles.

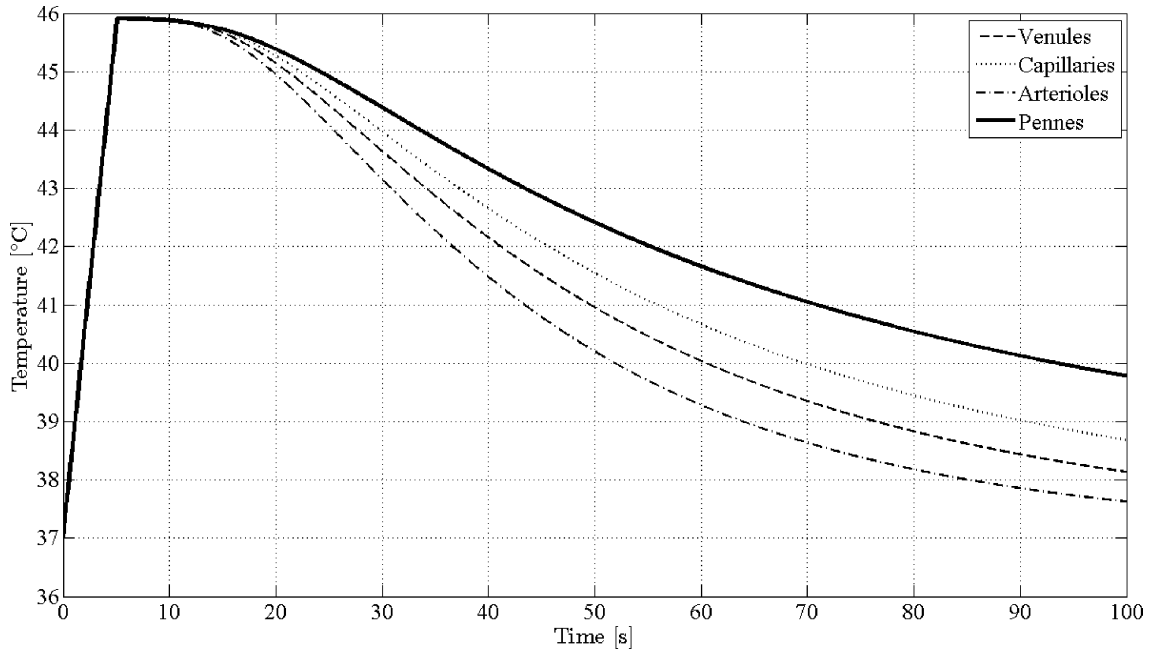


Fig. 6. Temperature history at the central point – 1st variant of heating.

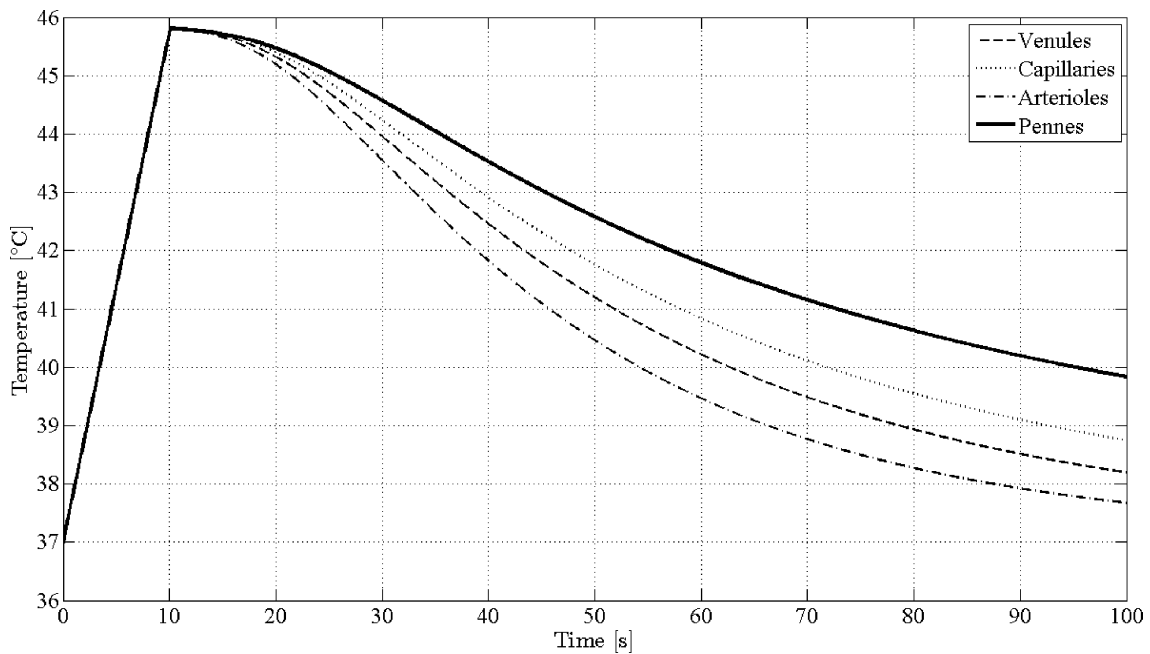


Fig. 7. Temperature history at the central point – 2nd variant of heating.

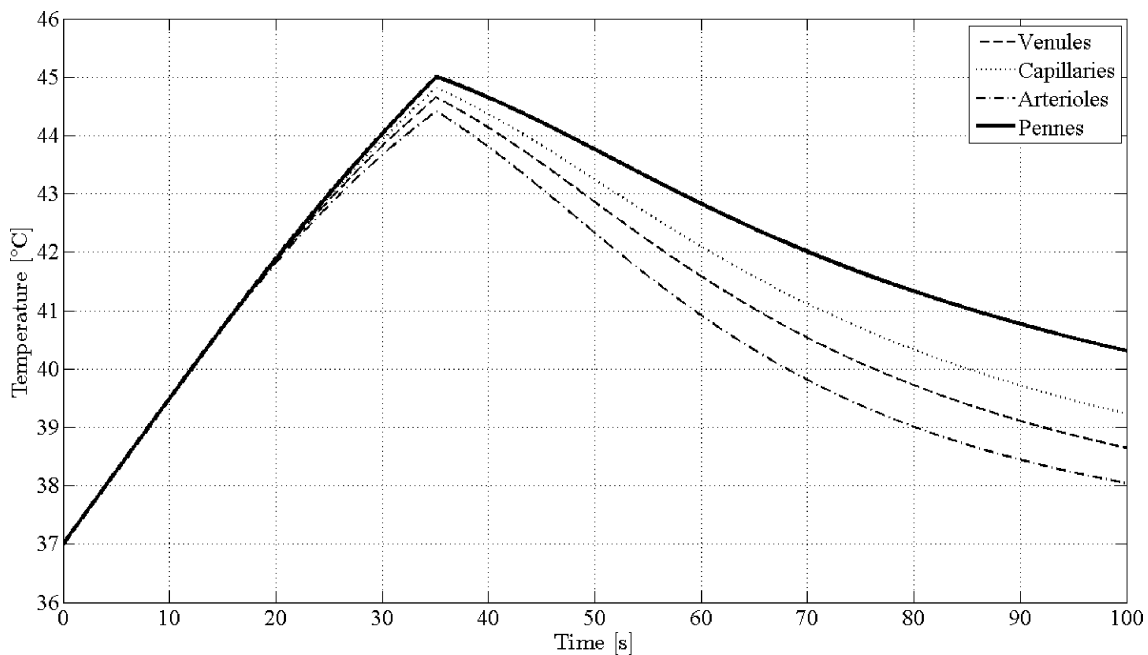


Fig. 8. Temperature history at the central point – 3rd variant of heating.

5. CONCLUSIONS

The 3D domain including healthy tissue and tumor region has been considered. The solutions obtained using different models of bioheat transfer are similar from the qualitative point of view but the differences between the temperature distributions are essential. However, for hyperthermia treatment more important is the estimation of proper time of heating assuring the destruction of tumor than the slight temperature difference. For a patient, long duration of heating at elevated temperature will induce a feeling of discomfort and pain, therefore the choice of heating variant is the most important. Based on the received temperature distributions the importance of porosity and blood flow velocity should be emphasized. Heating duration is also very important for the effectiveness of hyperthermia treatment. However, as can be seen from the presented results, the most important is the proper selection of a mathematical model.

ACKNOWLEDGEMENTS

The paper is a part of the project sponsored by the National Science Centre DEC 2011/01/N/ST6/05231.

REFERENCES

- [1] N. Afrin, Y. Zhang, J.K. Chen. Thermal lagging in living biological tissue based on nonequilibrium heat transfer between tissue, arterial and venous bloods. *International Journal of Heat and Mass Transfer*, **54**: 2419–2426, 2011.
- [2] C. Cattaneo. A form of heat conduction equation which eliminates the paradox of instantaneous propagation. *Comp. Rend.*, **247**: 431–433, 1958.
- [3] M. Ciesielski, B. Mochacki. Numerical analysis of interactions between skin surface temperature and burn wound shape. *Scientific Research of Institute of Mathematics and Computer Science*, **1**(11): 15–22, 2012.
- [4] G. Comini, L. Del Giudice. Thermal aspects of cryosurgery. *Journal of Heat Transfer*, **98**: 543–549, 1976.
- [5] K. Erhart, E. Divo, A. Kassab. An evolutionary-based inverse approach for the identification of non-linear heat generation rates in living tissues using localized meshless method. *International Journal of Numerical Methods for Heat and Fluid Flow*, **18**(3): 401–414, 2008.

- [6] W. Kaminski. Hyperbolic heat conduction equation for materials with a nonhomogeneous inner structure. *Journal of Heat Transfer*, **112**: 555–560, 1990.
- [7] A.R.A. Khaled, K. Vafai. The role of porous media in modeling flow and heat transfer in biological tissues. *International Journal of Heat and Mass Transfer*, **46**: 4989–5003, 2003.
- [8] J. Liu, L.X. Xu. Boundary information based diagnostics on the thermal states of biological bodies. *Journal of Heat and Mass Transfer*, **43**: 2827–2839, 2000.
- [9] E. Majchrzak. Numerical modelling of bio-heat transfer using the boundary element method. *Journal of Theoretical and Applied Mechanics*, **2**(36): 437–455, 1998.
- [10] E. Majchrzak. Numerical solution of dual phase lag model of bioheat transfer using the general boundary element method. *CMES: Computer Modeling in Engineering and Sciences*, **69**(1): 43–60, 2010.
- [11] E. Majchrzak, M. Dziewoński. Numerical simulation of freezing process using the BEM. *Computer Assisted Mechanics and Engineering Sciences*, **7**: 667–676, 2000.
- [12] E. Majchrzak, B. Mochnacki. *Numerical methods. Theoretical bases, practical aspects and algorithms*. Publ. of the Silesian University of Technology, Gliwice, Poland, 2004.
- [13] E. Majchrzak, J. Poteralska, Ł. Turchan. Comparison of different bioheat transfer models used in numerical modelling of a hyperthermia therapy. *International Conference of the Polish Society of Biomechanics “Biomechanics 2010”*, Book of Abstracts, 137–138, Warsaw, Poland, 2010.
- [14] E. Majchrzak, Ł. Turchan. Numerical modeling of a hyperthermia therapy using dual-phase-lag model of bioheat transfer. *19th International Conference on Computer Methods in Mechanics CMM 2011*, Short Papers, 337–338, Warsaw, Poland, 2011.
- [15] B. Mochnacki, M. Dziewoński. Numerical analysis of cyclic freezing. *Acta of Bioengineering and Biomechanics*, **6**(1): 476–479, 2004.
- [16] B. Mochnacki, E. Majchrzak. Sensitivity of the skin tissue on the activity of external heat sources. *CMES: Computer Modeling in Engineering and Sciences*, **4**(3–4): 431–438, 2003.
- [17] A. Nakayama, F. Kuwahara. A general bioheat transfer model based on the theory of porous media. *International Journal of Heat and Mass Transfer*, **51**: 3190–3199, 2008.
- [18] T. Peng, D.P. O’Neill, S.J. Payne. A two-equation coupled system for determination of liver tissue temperature during thermal ablation. *International Journal of Heat and Mass Transfer*, **54**: 2100–2109, 2011.
- [19] H.H. Pennes. Analysis of tissue and arterial blood temperatures in the resting human forearm. *Journal of Applied Physiology*, **1**: 93–122, 1948.
- [20] W. Shen, J. Zhang, F. Yang. Modeling and numerical simulation of bioheat transfer and biomechanics in soft tissue. *Mathematical and Computer Modelling*, **41**: 1251–1265, 2005.
- [21] P. Vernotte. Les paradoxes de la theorie continue de l’equation de la chaleur. *Comp. Rend.*, **246**: 3154–3155, 1958.
- [22] F. Xu, K.A. Seffen, T.J. Lu. Non-Fourier analysis of skin biothermomechanics. *International Journal of Heat and Mass Transfer*, **51**: 2237–2259, 2008.
- [23] P. Yuan. Numerical analysis of temperature and thermal dose response of biological tissues to thermal non-equilibrium during hyperthermia therapy. *Medical Engineering & Physics*, **30**: 135–143, 2008.
- [24] F. Xu, K.A. Seffen, T.J. Lu. Non-Fourier analysis of skin biothermomechanics. *International Journal of Heat and Mass Transfer*, **51**: 2237–2259, 2008.
- [25] J. Zhou, J.K. Chen, Y. Zhang. Dual-phase lag effects on thermal damage to biological tissues caused by laser irradiation. *Computers in Biology and Medicine*, **39**: 286–293, 2009.